

# Performance Characteristics of Digital Current Detector in DC-DC Converter

Yudai Furukawa, Shusuke Maeda and Fujio Kurokawa  
 Graduate School of Engineering  
 Nagasaki University  
 Nagasaki, Japan  
 bb52215203@cc.nagasaki-u.ac.jp

Ilhami Colak  
 Faculty of Engineering and Architecture  
 Gelisim University  
 Istanbul, Turkey  
 icolak@gelisim.edu.tr

**Abstract**— The purpose of this paper is to present a performance characteristics of digital current detector in dc-dc converter. The digital peak current mode control dc-dc converter using the voltage-controlled oscillator (VCO) has already proposed. The peak current is detected by using VCO in the proposed method. The gain of amplifier in the current detector affects to the input voltage range of VCO. Also, it affects the transient response. They are discussed by analysing and simulation.

**Keywords**—digital control, peak current mode control, dc-dc converter, digital current detector

## I. INTRODUCTION

In the recent year, the amount of information of server in the data center continues to increase. Therefore, the energy management in data center is very important. The digital control dc-dc converter has attracted attention because it has many advantages such as the energy management, the high performance control and the monitoring task [1]-[7]. The digital control circuit is consisted of the A-D converter and the operation derives. The delay time by the conversion time and the operation time exists in the digital control circuit and it adversely affects the transient response of the system. A digital current mode control method is effective for the improvement of the transient response.

However, when the digital peak current mode control is implemented, a high-speed A-D converter, which is expensive, is required in order to capture the peak current value correctly. The digital controller is also required a high-speed processing enough to turn off signal of the PWM at the timing when the current reaches the peak value. Therefore, implementing the peak current mode control by digital technology is difficult.

The authors have already proposed the digital peak current mode control circuit that does not require the high performance equipment [8, 9]. The proposed circuit converts the current value into the FM pulse by using the inexpensive voltage controlled oscillator (VCO). So that, it is possible to capture the peak current using the digital logic circuit, the programmable delay circuit and VCO. The comparison of

the conventional method in the transient response has already performed. The analysis of controller of proposed circuit is already derived [10].

This paper presents the transient response in changing characteristics of the current detector. The parameter of the amplifier of the current detector contains the derived control gains. We change the current gain and compare the transient of the output voltage respectively by using the simulation.

## II. OPERATION PRINCIPLE

Figure 1 shows the circuit configuration of the digital peak current mode control dc-dc converter. The main circuit is composed of the buck type dc-dc converter. In where,  $E_i$  is the input voltage,  $e_o$  is the output voltage,  $R$  is the load resistance,  $i_{T_r}$  is the switching current,  $R_s$  is the resistor to detect the switching current,  $D$  is the diode,  $L$  is the inductance  $C$  is the output capacitance  $i_L$  is the reactor current  $T_r$  is the switch and  $S_{T_r}$  is PWM signal. The proposed method uses  $i_{T_r}$  instead of  $i_L$  to reduce the loss while  $T_r$  is off.  $e_o$  detected from the main circuit is inputted to the digital control circuit through a preamplifier. The

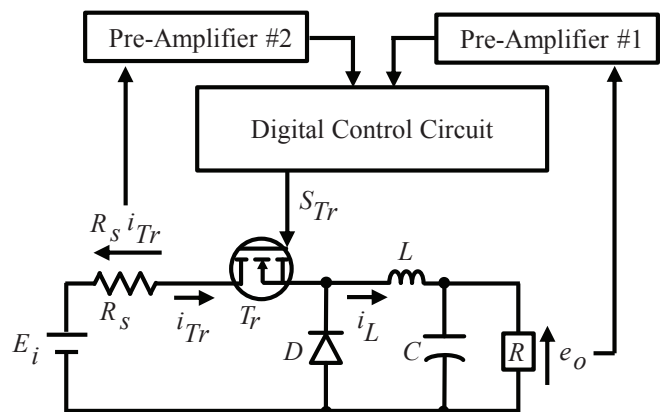


Fig. 1. Circuit configuration of digital peak current mode control dc-dc converter.

voltage  $R_s i_{Tr}$  that is equivalent to the switch current detected by the detection resistor is also inputted to the digital control circuit through a preamplifier.  $S_{Tr}$  is generated by the digital control circuit using these values.

Figure 2 illustrates the circuit configuration of digital control circuit.  $e_o$  is inputted to A-D converter through the preamplifier.  $A_{eo}$  is the gain of the preamplifier of  $e_o$ . The amplified voltage  $A_{eo}e_o$  is converted to the digital value  $e_o[n]$  and is inputted to the delay circuit as the calculation results of PID controller  $N_{PID}$ .  $R_s i_{Tr}$  is inputted to VCO through the preamplifier of  $R_s i_{Tr}$ .  $A_{iTr}$  is the gain of the preamplifier of  $R_s i_{Tr}$ . VCO is an element, which outputs the pulse frequency modulation (PFM) signal. The output signal  $S_f$  of VCO and the signal  $S_{fd}$ , that  $S_f$  is delayed by a delay

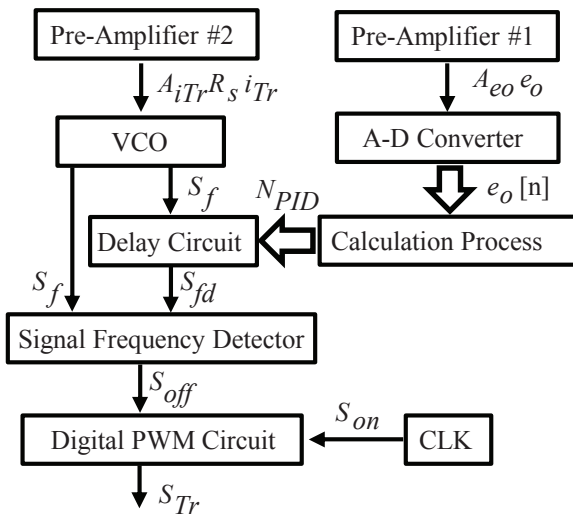


Fig. 2. Circuit configuration of digital control circuit.

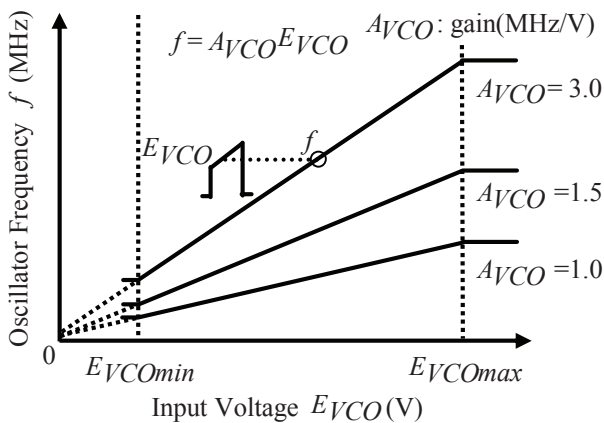


Fig. 3. Input-output characteristic of VCO.

circuit, are sent to the signal frequency detector. In the signal frequency detector, the timing of the turn off signal of the PWM is determined by  $S_f$  and  $S_{fd}$ . The signal of the turn on signal  $S_{on}$  of the PWM is sent by the CLK. PWM signal  $S_{Tr}$  is determined by this process.

The input-output characteristic of VCO is depicted in Fig. 3. The voltage  $E_{VCO}$  is inputted to VCO.  $E_{VCOmax}$  and  $E_{VCOmin}$  are the maximum value and minimum value, respectively.  $E_{VCO}$  is expressed by (1).

$$E_{VCO} = A_{iTr} R_s i_{Tr} (T_{on}) + E_B \quad (1)$$

where  $A_{iTr}$  is the gain of the preamplifier of detected current,  $i_{Tr}(T_{on})$  is the switch current in on period and  $E_B$  is the bias voltage. VCO outputs the oscillatory frequency. The relation of the input voltage and oscillatory frequency is obtained by (2).

$$T_f = \frac{1}{f} = \frac{1}{A_{VCO} \{A_{iTr} R_s i_{Tr} (T_{on}) + E_B\} + B} \quad (2)$$

where  $T_f$  is the one period of  $S_f$ ,  $f$  is the oscillatory frequency,  $A_{VCO}$  is the gain of VCO and  $B$  is the intercept of VCO characteristic. VCO is the characteristic that outputs the oscillatory frequency proportional to the input voltage.  $E_{VCO}$  linearly increases in the proposed method. So,  $f$  is gradually increased and  $T_f$  is decreased.

Figure 4 shows the timing chart of digital peak current detector. While  $S_{Tr}$  is on,  $i_{Tr}$  is linearly increased. Therefore,  $T_f$  is also gradually shortened.  $Q_1$  is the signal preset by the output voltage control loop and is equal to the delay time  $\tau$  in the signal frequency detector.  $\tau$  is obtained by (3).

$$\tau = T_D \cdot N_{PID} \quad (3)$$

where  $T_D$  is the resolution of delay buffer per one. The turn

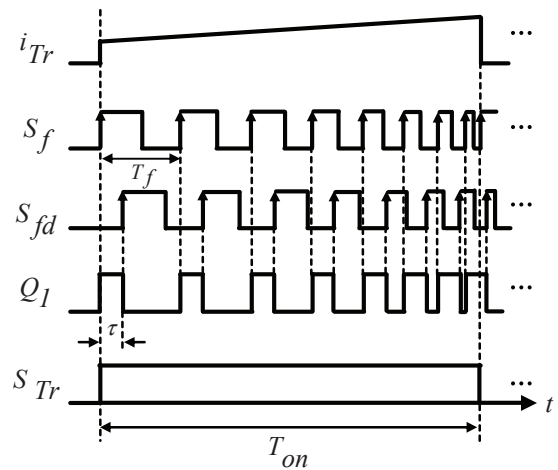


Fig. 4. Timing chart of digital peak current detector.

off of  $S_{Tr}$  is determined by the signal frequency detector using  $S_f$  and  $S_{fd}$ . The following equation is established when the signal frequency detector outputs the turn off signal.

$$\tau = T_f \quad (4)$$

### III. ANALYSIS OF CONTROL GAINS

The control analysis derived by previous research. The peak value of the switch current  $i_{Tr}(Ton)$  in the main circuit is obtained by (5).

$$i_{Tr}(Ton) = \frac{V_L}{L} T_{on} + I_L(0) \quad (5)$$

where  $V_L$  is the voltage of inductance while the switch is on  $T_{on}$  is an on time of the main switch and  $I_L(0)$  is the initial value of the inductor current. Here, the relational equation (6) of the current detector and the voltage detector is obtained by using (2), (3) and (4).

$$T_D \cdot N_{PID} = \frac{1}{A_{VCO} \{ A_{iTr} R_s i_{Tr}(Ton) + E_B \} + B} \quad (6)$$

$R_s A_{iTr} A_{VCO}$  in (6) is normalized as follows:

$$A_{ICO} = R_s A_{iTr} A_{VCO} \quad (7)$$

$A_{ICO}$  is the current gain. The equation (8) is derived by using (5) and (6). The equation (8) represents the equation of  $T_{on}$  by the output voltage detector and the current detector.

$$\frac{\Delta T_{on}(s)}{T_s} = \left\{ H_{PV} + sH_{DV} + \frac{H_{IV}}{s} \right\} \Delta e_o(s) - H_{PI} \Delta I_L(s) \quad (8)$$

$H_{PV}$  is the proportional gain,  $H_{IV}$  is the integral gain,  $H_{DV}$  is the differential gain and  $H_{PI}$  is the current gain in (8). The control gains in (8) derived by previously research are expressed by the following equations.

$$H_{PV} = \frac{2LA_{eo}G_{AD}f_s K_{PV}}{V_L A_{ICO} T_D N_{PID}^2} \quad (9)$$

$$H_{IV} = \frac{2LA_{eo}G_{AD}f_s^2 K_{IV}}{V_L A_{ICO} T_D N_{PID}^2} \quad (10)$$

$$H_{DV} = \frac{2LA_{eo}G_{AD}K_{DV}}{V_L A_{ICO} T_D N_{PID}^2} \quad (11)$$

$$H_{PI} = \frac{L f_s}{V_L} \quad (12)$$

where  $A_{eo}$  is the gain of pre-amplifier,  $G_{AD}$  is the gain of A-D converter and  $f_s$  is the switching frequency.  $K_{PV}$ ,  $K_{IV}$  and  $K_{DV}$  are coefficients of the P control, the I control and the D control, respectively.

### IV. SIMULATION RESULTS

Figure 5 illustrates the input-output characteristics of VCO in the simulation. The range of input voltage is varied by changing the value of  $A_{iTr}$ . The ranges I, II and III shown in Fig. 5 are  $A_{ICO} = 5.9$  (MHz / A),  $A_{ICO} = 2.9$  (MHz / A) and  $A_{ICO} = 2.0$  (MHz / A), respectively. The transient responses are compared with each range.

Figures 6, 7 and 8 show the result of the transient response of  $e_o$  and  $i_L$  by using the simulation. The step change of the load resistance is from  $10 \Omega$  to  $5 \Omega$ . As the main circuit parameter,  $E_i$  is 20 V,  $e_o$  is 5 V, the switching frequency is 100 kHz, the L is 194  $\mu$ H, the output capacitance is 990  $\mu$ F,  $R_s$  is 0.05  $\Omega$  and R is 5  $\Omega$ .  $K_{PV}$ ,  $K_{IV}$

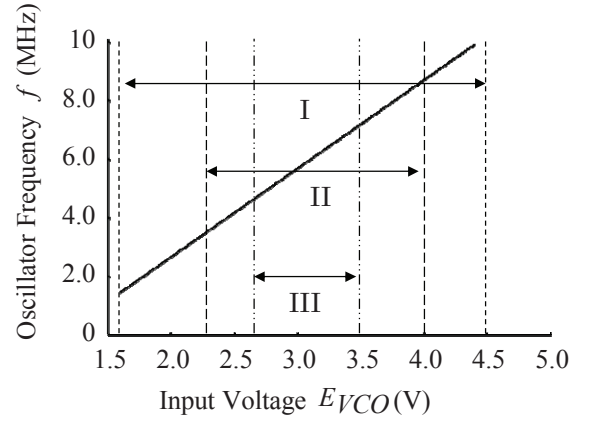


Fig. 5. Input-output characteristic of VCO in simulation.

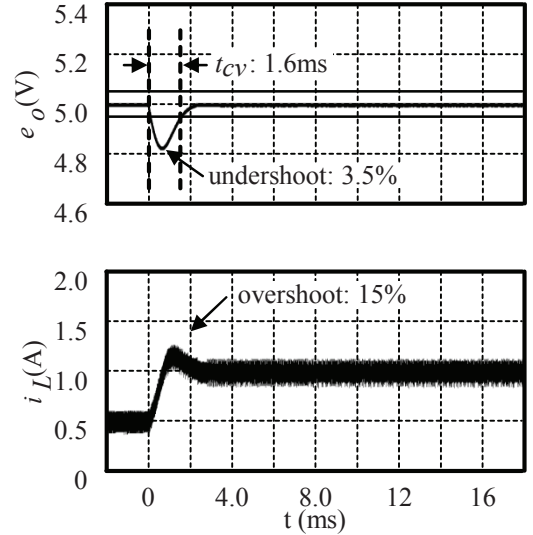


Fig. 6. Transient responses of  $e_o$  and  $i_L$  taking  $A_{ICO} = 5.9$  (MHz / A) as a parameter.

and  $K_{DV}$  are equal to 3, 0.05 and 1, respectively. The difference among Figs. 6, 7 and 8 is the value of  $A_{ICO}$ .  $A_{ICO}$  is varied by changing the value of  $A_{ITr}$  and the value of  $A_{VCO}$  is fixed. The value of  $A_{ICO}$  is equal to 5.9 (MHz/A) in Fig. 6. The convergence time  $t_{cv}$ , the undershoot and the overshoot are 1.6 ms, 3.5% and 15%, respectively. In Fig. 7, the value of  $A_{ICO}$  is equal to 2.9 (MHz/A).  $t_{cv}$ , the undershoot and the overshoot are 0.8 ms, 1.6% and 8.6%, respectively. Comparing Fig. 7 with Fig. 6,

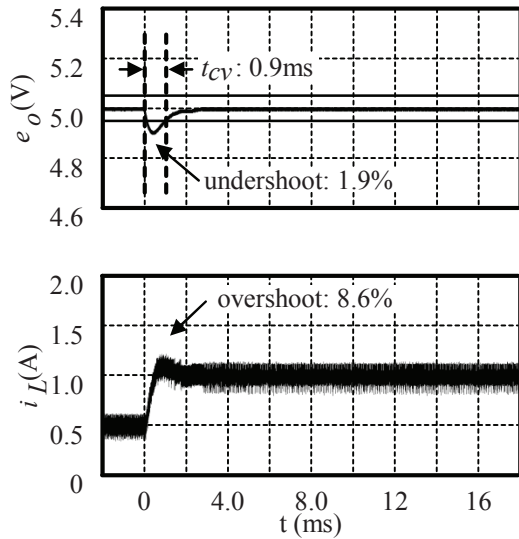


Fig. 7. Transient responses of  $e_o$  and  $i_L$  taking  $A_{ICO} = 2.9$  (MHz/A) as a parameter.

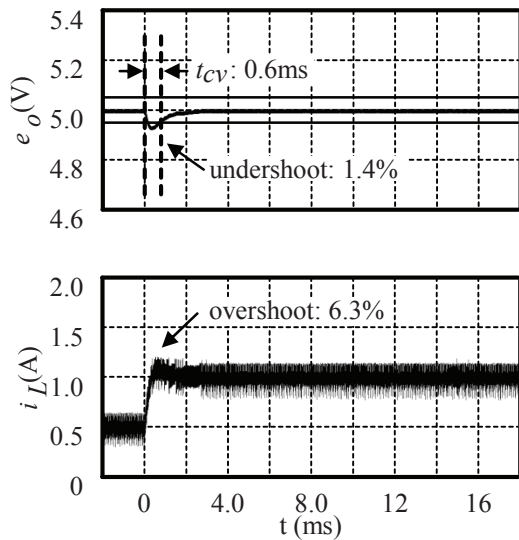


Fig. 8. Transient responses of  $e_o$  and  $i_L$  taking  $A_{ICO} = 2.0$  (MHz/A) as a parameter.

the control gains are doubled. So,  $t_{cv}$ , the undershoot and the overshoot are improved by 44%, 46% and 43%, respectively. In Fig. 8, the value of  $A_{ICO}$  is equal to 2.0 (MHz/A).  $t_{cv}$ , undershoot and overshoot are 0.6 ms, 1.4% and 6.3%, respectively. Comparing Fig. 8 with Fig. 6, the control gains are tripled.  $t_{cv}$ , the undershoot and the overshoot are improved by 63%, 60% and 58%, respectively.

## V. CONCLUSION

This paper presents the performance characteristics of the current detector in the digital peak current mode dc-dc converter using VCO. The control gains in the proposed method are also derived. It is discussed that the effect of the value of  $A_{ICO}$  affects the transient response. A superior transient response is obtained when the value of  $A_{ICO}$  is 2.0 (MHz/A) compared with the case of  $A_{ICO} = 5.9$  (MHz/A).  $t_{cv}$ , the undershoot and the overshoot are improved by 63%, 60% and 58%, respectively, in Fig. 6 and Fig. 8. When smaller value of  $A_{ICO}$  is set, it is possible to obtain a better transient response. Although the transient response is improved by the smaller value of  $A_{ICO}$ , the resolution of the current detector is also changed and becomes coarse. Therefore, the proper value should be set to meet both the transient and static characteristics.

## REFERENCES

- [1] S. Strache, J. H. Mueller, R. Wunderlich and S. Heinen, "Advanced digital current prediction for current ripple reduction in dc-dc converters for photovoltaic applications," the Proc. the IEEE IECON, pp. 6968-6973, November, 2013.
- [2] S. Effler, Z. Lukic and A. Prodic, "Oversampled digital power controller with bumpless transition between sampling frequencies," in Proc. the IEEE Energy Conversion Congress and Exposition, pp. 3306-3311, September, 2009.
- [3] V. Arikatla and A. A. Qahouq, "DC-DC power converter with digital PID controller," in Proc. the IEEE Applied Power Electronics Conference and Exposition, pp. 327-330, March, 2011.
- [4] P. Zumel, C. Fernández, M. Sanz, A. Lazaro and A. Barrado, "Simple configurable digital compensator for dc-dc power converters," in Proc. the IEEE Applied Power Electronics Conference and Exposition, pp. 1208-1214, February, 2009.
- [5] S. Saggini, A. Costabeber, and P. Mattavelli "A simple digital autotuning for analog controller in SMPS," Trans. on IEEE Power Electronics, vol. 25, no. 8, pp. 2170-2178, August 2010.
- [6] S. Saggini, A. Costabeber, and P. Mattavelli "A simple digital autotuning for analog controller in SMPS," Trans. on IEEE Power Electronics, vol. 25, no. 8, pp. 2170-2178, August 2010.
- [7] C. H. Tsai, C. H. Yang, J. H. Shiau and B. T. Yeh, "Digitally controlled switching converter with automatic multimode switching," Trans. on IEEE Power Electronics, vol. 29, no. 4, pp. 1830-1839, April, 2014.
- [8] F. Kurokawa and Y. Komichi, "A new peak-current injected digital control circuit for dc-dc converter," in Proc. the IEEE Power Electronics and Applications, pp. 1-7, August, 2011.
- [9] F. Kurokawa, H. Tamenaga, Y. Shibata and Y. Yamabe "Regulation characteristics of fast response digitally peak current controlled dc-dc converter," in Proc. the IEEE Power Electronics and Drive Systems, pp. 1114-1118, April, 2013.
- [10] F. Kurokawa, S. Maeda and Y. Furukawa, "Analysis of digital peak current control dc-dc converter," in Proc. the IEEE Renewable Energy Research and Application, pp. 737-742, October, 2014.